EUKARYOTIC CELL, June 2009, p. 858–866 Vol. 8, No. 6
1535-9778/09/$08.00+0 doi:10.1128/EC.00017-09

Isolation and Characterization of Senescent *Cryptococcus neoformans* and Implications for Phenotypic Switching and Pathogenesis in Chronic Cryptococcosis▽

Neena Jain,[1] Emily Cook,[1] Immaculata Xess,[2] Fahmi Hasan,[2] Dietrich Fries,[3] and Bettina C. Fries[1]*

Departments of Medicine and Microbiology and Immunology, Albert Einstein College of Medicine, Bronx, New York 10461[1]; Department of Microbiology, All India Institute of Medical Sciences, New Delhi, India[2]; and Institute für Experimentale Kernphysik, Universität Karlsruhe, Karlsruhe, Germany[3]

Received 12 January 2009/Accepted 17 April 2009

Although several virulence factors and associated genes have been identified, the mechanisms that allow *Cryptococcus neoformans* to adapt during chronic infection and to persist in immunocompromised hosts remain poorly understood. Characterization of senescent cells of *C. neoformans* demonstrated that these cells exhibit a significantly enlarged cell body and capsule but still cross the blood-brain barrier. *C. neoformans* cells with advanced generational age are also more resistant to phagocytosis and killing by antifungals, which could promote their selection during chronic disease in humans. Senescent cells of RC-2, a *C. neoformans* strain that undergoes phenotypic switching, manifest switching rates up to 11-fold higher than those of younger cells. Infection experiments with labeled cells suggest that senescent yeast cells can potentially accumulate in vivo. Mathematical modeling incorporating different switching rates demonstrates how increased switching rates promote the emergence of hypervirulent mucoid variants during chronic infection. Our findings introduce the intriguing concept that senescence in eukaryotic pathogens could be a mechanism of microevolution that may promote pathoadaptation and facilitate evasion of an evolving immune response.

Cryptococcus neoformans is an encapsulated yeast that causes chronic meningoencephalitis predominantly in patients with advanced human immunodeficiency virus infection. Worldwide, this disease is estimated to cause more than 600,000 deaths per year (22). This high death rate may result in part from the fact that this chronic infection is notoriously difficult to eradicate, despite effective antifungal therapy. Even in successfully treated patients with access to antiretroviral therapy, the organism persists and can cause relapse both before and after the start of highly active antiretroviral treatment.

In murine infection models, *C. neoformans* strain RC-2 can augment virulence by undergoing phenotypic switching from a smooth (SM) parent colony to a more virulent mucoid (MC) colony variant (6). Phenotypic switching occurs in both species and varieties of this fungus (6, 8, 11). Although differentially regulated genes associated with switching have been described (10), the precise molecular mechanism that controls phenotypic switching in *C. neoformans* is unknown. In vitro investigations have demonstrated that phenotypic switching occurs at a stable rate and MC switch variants spontaneously arise at a rate of 1 in about 20,000 plated SM colonies. Environmental signals that induce or alter this process have not been identified to date. Phenotypic switching occurs during chronic murine infection and alters the outcome (6), but it is noteworthy that MC switch variants consistently emerge late in the course of infection (after 6 weeks), although the fungal burden is highest on day 14 after intratracheal (i.t.) infection. This could reflect altering selection pressure by an evolving host response or, alternatively, a change in the microbe's propensity to undergo phenotypic switching over time. In *Candida albicans*, the process of phenotypic switching is controlled by pathways that are involved in silencing and maintenance of genomic stability (14, 20, 34, 35). Furthermore, in the context of research on aging in *Saccharomyces cerevisiae*, it has become evident that senescent yeast cells (old cells with advanced generational age) exhibit less genomic stability (17, 18). *C. neoformans* is also a unicellular haploid yeast that replicates clonally in vivo. Consequently, we reasoned that it was conceivable that replicative aging of *C. neoformans* during chronic infection could alter genomic stability and its propensity to undergo phenotypic switching. We therefore investigated the effect of generational aging on phenotypic switching in *C. neoformans* and also compared it to *C. albicans*.

MATERIALS AND METHODS

***C. neoformans* and *C. albicans* strains.** RC-2 is a variant of the serotype D strain 24067 generated in our laboratory (3). Strain 24067 was originally obtained from the American Type Culture Collection (Manassas, VA). The RC-2 strain can produce two colony morphologies on Sabouraud dextrose agar (SDA) plates known as SM and MC, both of which are characteristic of *C. neoformans* colonies. *C. albicans* strain WO-1 switches between white and opaque colony morphologies as described previously (27). *C. neoformans* was grown in standard Sabouraud dextrose (SDB) and synthetic dextrose (SD) media (6.7 g Bacto yeast nitrogen base without amino acids and 20 g glucose per liter). Also, SD+ medium [SD medium supplemented with 0.4% ethanol, 5 g $(NH_4)_2SO_4$ per liter, and 3.3 g NaCl per liter] was used because it inhibits capsule expression. WO-1 was grown in Lee's medium (13), and switching was assessed on agar plates supplemented with 5 mg/liter phloxine B as described previously (31).

Isolation of senescent *C. neoformans* cells. A method to isolate *C. neoformans* cells with advanced generational age was developed on the basis of previously published protocols for *S. cerevisiae* (12, 25). *C. neoformans* RC-2 cells were grown overnight in SD medium. Because larger polysaccharide capsules interfere with the isolation of senescent cells, the overnight culture was diluted 1:50 and

* Corresponding author. Mailing address: Albert Einstein College of Medicine, Ullmann 1223, 1300 Morris Park Ave., Bronx, NY 10461. Phone: (718) 430-2365. Fax: (718) 430-8968. E-mail: fries@aecom.yu.edu.

▽ Published ahead of print on 1 May 2009.

grown for approximately 6 h in SD+ medium. Under these growth conditions, the mean thickness of the polysaccharide capsule was less than 1 μm. Counterflow centrifugal elutriation was performed to isolate newly budded cells (<5 μm in diameter). This method isolates fractions of different-sized cells on the basis of their sedimentation coefficient, which is a function of cell volume and density. A cell suspension (1×10^8 to 5×10^8 yeast cells) was loaded at 14 ml/min into a rotating elutriator rotor (Beckman JE-5.0 in a Beckman J-6B centrifuge; Beckman Instruments Inc., Palo Alto, CA) while the rotor speed was kept constant at 3,500 rpm. Cells were collected in 100-ml fractions at increasing flow rates with a peristaltic pump. The flow rates were 16 ml/min, 20 ml/min, and 25 ml/min for fractions 1 to 3, respectively. The first two fractions contained small *C. neoformans* cells (<5 μm; generation 0). Generation 0 cells were washed one time, suspended in phosphate-buffered saline (PBS) at 5×10^7/ml, and labeled at room temperature with biotin (Sulfo-NHS-LC-biotin; Pierce, Rockford, IL) at a concentration of 4 mg/ml in PBS. These cells constituted the starting population from which we derived old cells of advanced generational age. This label is unable to permeate the cell membrane and thus labels only surface proteins and can be visualized by staining with fluorescein streptavidin conjugate (Molecular Probes Inc., Eugene, OR). Biotin-labeled cells retain the label and exhibit normal function and a normal growth rate. Cells were washed five times with PBS, and positive staining was confirmed in a small fraction before cells were grown overnight in SDB. After approximately five or six doubling times, they were washed in PBS, resuspended at 10^7/90 μl, and incubated with 10 μl streptavidin-conjugated magnetic microbeads (Miltenyi Biotec, Auburn, CA) for 15 min at 6 to 10°C. Magnetic-bead-labeled cells were washed, resuspended at 10^8/500 μl PBS, and isolated via a LS magnetic column (Miltenyi Biotec). The retained bead-positive cell fraction was released by disrupting the magnetic field. The purity of the positive cells was confirmed by staining, and the cells were reintroduced into overnight culture as described above. The procedure was repeated four or five times to isolate senescent (18 to 30 generations old) cells. With increasing isolation, a significant percentage of the cells (>50%) was lost. Notably, restaining and relabeling of the positive cells after two rounds (10 generations) could increase the yield. For *C. albicans*, the same protocol was applied. The initial elutriation step was not required for *Candida* cells, as they lack a capsule. To verify the generational age of isolated cells, the input and output cells were carefully counted and the doubling times and generations were mathematically inferred. Fluorescent staining of total populations was used as an independent confirmation of the result (percentage of green fluorescent cells).

Switching frequency. Phenotypic switching was defined as the spontaneous generation of colony variants with altered colony morphology (6). For calculation of switching frequencies, 200 to 300 cells with the SM "parent" phenotype were plated on 100 SDA plates and 10^4 colonies were scored for the respective MC "switch variant" phenotype. The percentage of the total number of CFU with MC morphology relative to the percentage with SM morphology was determined. For WO-1 cells, the white cells were plated on phloxine B-supplemented agar plates. The ratio of pink (opaque) to white (white) cells was calculated (29).

Phenotypic characterization of senescent cells and their detection in vivo. (i) Cell morphology and capsule size measurements. For capsule size measurements, senescent and young yeast cells were suspended in India ink (Becton Dickinson, Franklin Lakes, NJ) and visualized at ×1,000 magnification with an Olympus AX70 microscope. Images were captured with a QImaging Retiga 1300 digital camera with the QCapture Suite V2.46 software (QImaging, Burnaby, British Columbia, Canada). Capsule measurements were made on 25 to 40 randomly chosen cells of each strain with Adobe Photoshop 7.0 for Windows, and capsule thickness was calculated with the conversion of 15 pixels/μm, as described previously (33). Capsule of senescent cells was induced in vitro by incubating the cells at 37°C for 48 h in Dulbecco modified Eagle medium supplemented with 10% fetal calf serum (33). Bud scars were stained with fluorescein isothiocyanate (FITC)-conjugated wheat germ agglutinin (WGA) lectin in accordance with the manufacturer's protocol (Sigma-Aldrich). As a control, senescent *S. cerevisiae* cells (approximately 15 generations old) were stained with WGA.

(ii) In vivo detection. For in vivo staining, mice were sacrificed at day 14 and day 21 post i.t. infection with 10^6 cells (overnight culture biotin labeled). Single-cell suspensions were obtained from lung homogenates and stained with FITC-conjugated streptavidin to identify biotin-labeled cells. As a negative control, cells from mice infected with unlabeled cells were used. For a rough estimate of percentage of biotin-labeled cells, we counted all of the fungal cells under phase-contrast microscopy and then the FITC-positive cells under fluorescence microscopy.

(iii) Phagocytosis assay. For in vitro phagocytosis assays, J774.16 cells were grown in a 96-well tissue culture plate and young or old *C. neoformans* cells were added at a fungus-to-macrophage ratio of 1:1 in the presence of capsule-specific monoclonal antibody 18B7 (1 μg/ml). After 2 h, the cell layers were washed, fixed, and stained with Giemsa and the phagocytosis index (number of yeast cells in macrophages/number of macrophages) was determined. The assay was performed in triplicate, and a total of 500 macrophages per group were counted to calculate the phagocytosis index.

(iv) Karyotype analysis of senescent cells. Senescent cells (24 generations old) of both the SM parent (O) and MC switch (O*) phenotypes were regrown briefly for two or three generations to produce enough cells (>10^8) for the isolation of chromosomal DNA. Also, plugs were made from young cells (overnight culture). Plugs were prepared from cultures as described before (4). After washing, the plugs were inserted into a 1% pulsed-field-certified agarose gel (Bio-Rad, Richmond, CA) and electrophoresis was done in a CHEF DRIII variable-angle pulsed-field gel electrophoresis system (Bio-Rad) in 0.5% Tris-borate-EDTA at 12°C. The electrophoresis conditions were programmed in two sequential blocks (first a switch time of 90 s for 9 h and then switch times of 120 s and 360 s for 63 h). Both blocks were run at 3.5 V/cm at an angle of 115°. Gels were stained with ethidium bromide and photographed.

Killing assay. The in vitro killing efficiency of increasing doses of fluconazole, amphotericin B, and caspofungin was determined for young and old cells. Briefly, young and old cells were isolated as described above and diluted to 1×10^4/ml in RPMI 1640 medium (morpholinepropanesulfonic acid [MOPS] buffered to pH 7). Fluconazole, amphotericin B, or caspofungin was serially diluted in 100-μl volumes at concentrations of 128 to 1,000 μg/ml, 0.125 to 2 μg/ml, and 4 to 512 μg/ml, respectively, in RPMI medium buffered with MOPS in a 96-well plate. Volumes of 100 μl of young and old cells were added to achieve final concentrations of 5×10^3 cells/ml, 64 to 500 μg/ml fluconazole, 0.06 to 1 μg/ml amphotericin B, and 2 to 256 μg/ml caspofungin. Wells with no antifungal agent were included in the plate as controls. The plate was incubated at 37°C with shaking for 2.5 h (*C. neoformans*) and 4 h (*C. albicans*), and 100 μl of each well was plated on SDA plates and incubated at 37°C for 48 h. All experiments were performed in triplicate, and the killing percentage was calculated by comparison of antifungal-treated CFU count to the CFU count of the respective control (without antifungal treatment).

Animal studies. BALB/c mice (male, 6 to 12 weeks old) were obtained from the National Cancer Institute (Bethesda, MD). Groups of anesthetized mice (10 per group) were infected by i.t. inoculation of 10^5 old and young *C. neoformans* cells in 50 μl sterile, nonpyrogenic PBS with a 26-gauge needle as previously described (9). Dilutions of the infecting suspension were plated onto SDA plates to ensure that comparable numbers of viable yeast cells were injected. Mice were observed daily for signs of disease. Mice were killed by cervical dislocation after anesthesia, and organ fungal burdens were determined by homogenizing lung and brain tissues in 10 ml of PBS and plating 100-μl volumes of different dilutions of the homogenate on SDA (Difco Laboratories, Detroit, MI). Colonies were counted after 48 h (1 colony = 1 CFU). To compare in vivo crossing of the blood-brain barrier by young and old cells, intravenous (i.v.) infection was performed as described previously (11). Briefly, young and old cells were isolated as described above and BALB/c mice (five per group) were injected in the tail vein with 6×10^5 cells. The inoculum size was verified by back plating onto SDA plates. After 3 h, the mice were anesthetized and perfused with PBS and the brains were removed and homogenized in 2 ml of sterile PBS and plated on SDA plates to determine the number of CFU per brain.

Mathematical modeling. The time-dependent growth or (decrease) of biological populations can be mathematically represented by first-order differential equations (19). We devised a simple mathematical model for the growth of two classes of cells, *A* (SM) and *B* (MC), whose in vivo growth is influenced by the immune response as follows: $dA/dt = \alpha 1 \times A(t) \times H(t)$ for SM cells and $dB/dt = \beta 1 \times B(t) \times h(t)$ for MC cells. $A(t)$ and $B(t)$ represent the (unknown) number of cells at time t. dA/dt represents the change in the population size (A) at any time t [same for $B(t)$]. $H(t)$ and $h(t)$ are immune factors which modify the growth of $A(t)$ or $B(t)$. These factors are assumed to be a function of time t but might also be dependent on other parameters, such as the number of A or B cells (in this case, the equation depends on the square of A, or B would become nonlinear). $\alpha 1$ and $\beta 1$ are constants representing the growth rates. These differential equations can be solved numerically, yielding solutions $A(t)$ and $B(t)$. If H is constant (i.e., a number), the differential equations describe an exponential increase or decrease in the number of A or B cells in time (depending on the sign of $\alpha 1$). We have assumed for $H = H(t)$ that it is time dependent.

Statistical analysis. Standard statistical analyses, including the Kaplan-Meier test, log rank regression analysis, and the t test, were performed with the programs SPSS version 7.5.1 and Microsoft EXCEL version 11.5.3.

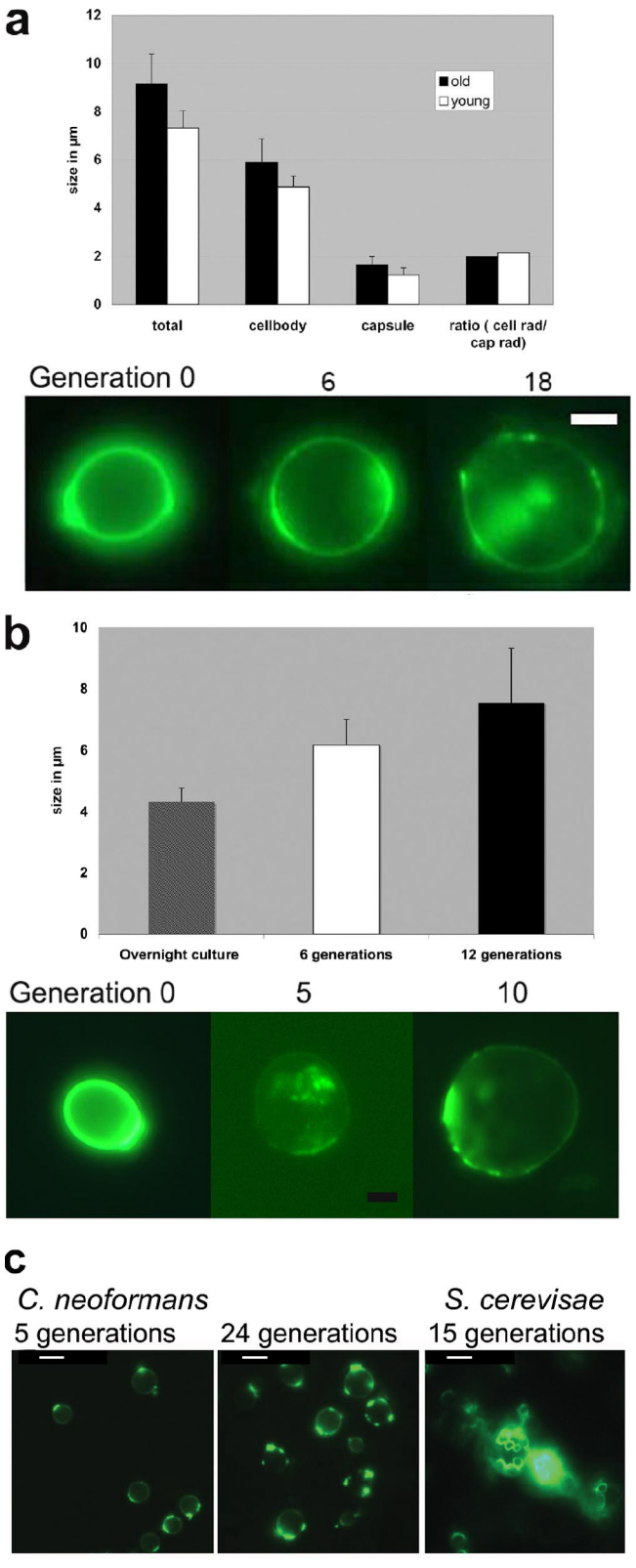

FIG. 1. Phenotypic characterization of senescent *C. neoformans* and *C. albicans* cells. (a) The larger size of 24-generation-old *C. neoformans* cells involves increases in both the capsule and the cell body. The increase is progressive over generations, as shown in FITC-stained, biotin-labeled cells. Bar size, 2 μm. (b) Similar size increases were seen in senescent *C. albicans* cells. Bar size, 2 μm. Notably, the biotin label faded more over time. (c) Staining with WGA lectin cannot be used to adequately determine the generation. Opposed to *S. cerevisiae* (right panel), the bud scars of *C. neoformans* appear to heal over or become undetectable with time. Bar size, 3 μm.

RESULTS

Isolation of senescent *C. neoformans* and *C. albicans* cells (Fig. 1). We successfully adapted published protocols for *S. cerevisiae* and developed a method to isolate senescent *C. neoformans* cells that were more than 30 generations old. In contrast to *C. neoformans* cells, we were not able to isolate senescent *Candida* cells that were older than 14 generations because *C. albicans* cells consistently transformed into a hyphal phenotype as they grew older. Hyphal cells could not be isolated by this strategy because the hyphae promoted clumping, which clotted the magnetic column and prevented flowthrough. The doubling time increased with generational age, and for *C. neoformans* cells older than 25 generations, it was about twice as long. Old cells of both *C. neoformans* and *C. albicans* were significantly larger than young cells ($P < 0.001$ by *t* test and analysis of variance). The size of *C. neoformans* biotin-positive cells was 9.1 ± 1.2 μm (24 generations), and that of biotin-negative cells was 7.3 ± 0.71 μm (overnight logarithmic culture) (Fig. 1a). The size of biotin-positive *C. albicans* cells was 6.2 ± 0.8 μm at 6 generations and 7.6 ± 1.7 μm at 12 generations, and that of biotin-negative cells from an overnight culture was 4.3 ± 0.4 μm (Fig. 1b). Notably, the biotin label faded much more rapidly in *C. albicans* than in *C. neoformans* (Fig. 1b). Also, the increase in *C. neoformans* cell size was proportional for the cell body and the capsule. Bud scar staining was performed with WGA, a lectin that preferably binds to bud scars. In contrast to *S. cerevisiae*, we detected no more than five bud scars per *C. neoformans* cell (Fig. 1c).

Increased switching rate in senescent *C. neoformans* cells (Fig. 2). Phenotypic switching rates were compared between young and old *C. neoformans* strain RC-2 cells. Prior to plating, we confirmed the 95% purity of senescent cells by staining with FITC-conjugated streptavidin. A dramatic increase in the switching rate between young and old cells was seen and confirmed in repeat experiments. The switching rate increased with age and was 6- and 11-fold greater in cells 27 and 31 generations old, respectively (Fig. 2b to d). Cells that were 15 generations old exhibited no significant increase in the switching rate. An effect of senescence on the switching of *C. albicans* strain WO-1 (30) could not be accurately determined because only cells up to 14 generations old could be isolated and the switching rate, which was determined by the color of colonies, was noted to be highly variable between experiments (data not shown). Comparison of the karyotype patterns of old *C. neoformans* cells with either SM colony morphology (O) or switched MC colony morphology (O*) demonstrated no detectable rearrangements in the karyotype pattern. However, changes in the second largest chromosome were seen in the karyotype patterns of both old cell types (O, O*). Their karyotype pattern appeared to have a wider or extra band in that chromosome compared to the karyotype pattern of young cells (Fig. 2a).

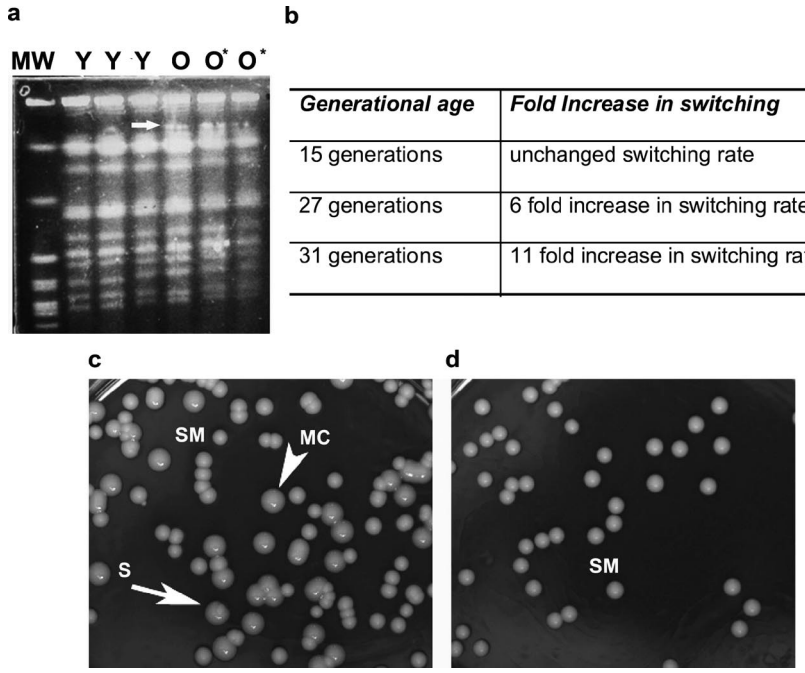

FIG. 2. Phenotypic switching rate is augmented in senescent RC-2 cells. (a) Karyotype analysis of young (Y) and old (O = old parent SM, O* = old switched MC) *C. neoformans* cells indicates changes in the chromosome 2 of old (O, O*) cells but no karyotype changes in old cells compared to young (Y) cells. (b, c, d) The rate of switching from SM to MC (arrowhead) increased with age, and many sectored colonies (arrow) were detected. MW, molecular weight markers.

Characterization of senescent cells in vivo (Fig. 3). Criteria to reliably identify senescent cells within a pathogen population are not available. Therefore, we took several indirect approaches to investigate these cells in vivo. First, we determined if the persistence of old cells occurs during chronic murine infection. For these experiments, mice were infected with biotin-labeled *C. neoformans* cells (overnight culture) and sacrificed at 14 and 21 days postinfection. At this time, the lung CFU count is highest in infected mice. Lung homogenates were stained with FITC-conjugated streptavidin to identify biotin-labeled cells. These cells would represent cells from the original inoculum that could have theoretically undergone up to 80 doubling times (assuming a 4-h doubling time) by day 14. Biotin-positive cells were detected in lung homogenates from mice infected for 14 and 21 days (Fig. 3a) in low numbers (approximately 1 to 10% of the extracellular yeast cells). In these lung homogenates, actively budding biotin-positive cells were also seen (Fig. 3a). Next, we compared the survival times of mice injected with young and old (24 generations) *C. neoformans* cells. This experiment documented comparable median survival times, specifically, 53 days versus 56 days in mice that were infected with young and old cells ($P = 0.6$) (Fig. 3b). Lastly, we compared the transmigration of young and old *C. neoformans* cells (18 generations) across the blood-brain barrier in mice infected i.v. These experiments documented that both old and young *C. neoformans* cells crossed the blood-brain barrier equally (Fig. 3c).

Enhanced resistance of senescent cells to antifungal therapy and phagocytosis (Fig. 4 and 5). To further investigate mechanisms that could facilitate the persistence and selection of senescent cells, we examined their resistance to killing by antifungal agents and to antibody-mediated phagocytosis by macrophages. Both assays are not dependent on the growth of *C. neoformans*. Senescent *C. neoformans* cells were more resistant to killing with therapeutic doses of amphotericin B, a lethal antifungal agent. At higher-than-therapeutic levels of fluconazole, a static antifungal agent, enhanced resistance to killing was also observed. For *C. albicans*, enhanced resistance to killing by caspofungin in therapeutic dose ranges was established. Furthermore, antibody-mediated phagocytosis of senescent *C. neoformans* cells was significantly ($P = 0.04$) decreased in comparison to the phagocytosis of young cells grown overnight. Capsule induction in vitro was also more pronounced in senescent *C. neoformans* cells (Fig. 5) but, relative to the enlarged cell body, comparable for old and young cells.

Mathematical modeling of the emergence of MC colonies in vivo as a result of altered switching rates (Fig. 6). The emergence of MC colonies was modeled according to biological data derived from two large murine infection experiments (5, 6) in which >100 mice were infected i.t. with 10^4 SM or MC CFU (5, 6). These experiments had demonstrated that mice infected i.t with 10^4 SM cells exhibited a lung CFU count of log 6.25 at day 14. These mice cleared the infection by day 140. In contrast, mice infected i.t with 10^4 MC cells exhibited a comparable lung CFU count of log 6.0 at day 14. MC cell-infected mice did not clear the infection (median survival time of 33 days and a lung CFU count of more than log 7). A simple mathematical model for the growth of *A* (SM) and *B* (MC) cells whose in vivo growth was influenced by the immune response was devised as outlined in Materials and Methods. The emergence of MC cells derived from

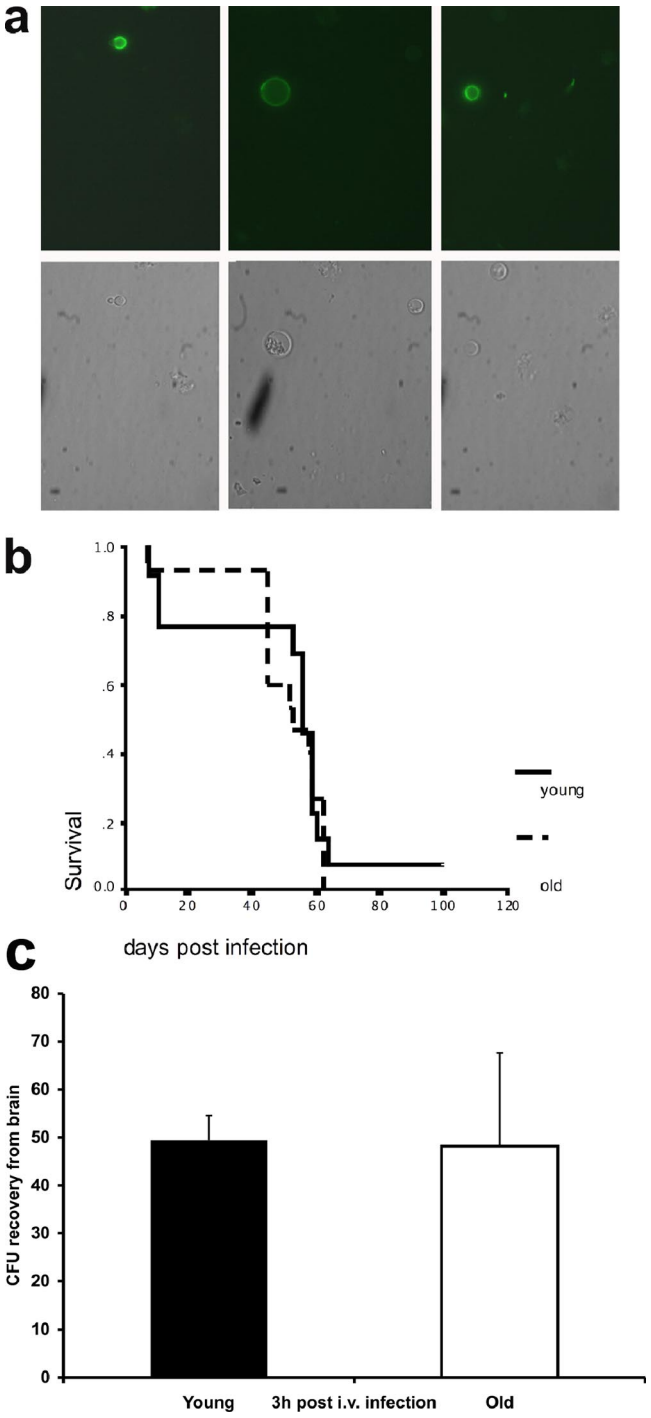

FIG. 3. In vivo detection, survival, and migration of senescent cells. (a) Biotin-positive cells in lung homogenates from mice infected for 14 days. Note that biotin-labeled, actively budding cells were observed in these lung homogenates (left). (b) No survival difference was documented in mice infected i.t with young (overnight culture) or old (24 generations) cells. (c) After i.v. infection, old (18 generations) and young *C. neoformans* cells crossed the blood-brain barrier equally.

switching of SM to MC at rates of 1:20,000 and 1:2,000 was modeled in parallel (Fig. 6), demonstrating that changes in switching rate without changes in host response would greatly affect the emergence of MC cells in vivo.

DISCUSSION

These data are the first to demonstrate the isolation and characterization of senescent *C. neoformans* cells. Our data suggest that *C. neoformans* cells that are more than 20 generations old are fit and could potentially accumulate during chronic infection. They exhibit enhanced resistance to antifungals and phagocytosis by macrophages. This could potentially promote their selection in patients who are treated with amphotericin B, and thus these cells may contribute to persistence of infection despite treatment with effective antifungals. In addition, in strain RC-2, senescence is associated with a significantly augmented switching rate to the hypervirulent MC phenotype, which could contribute as an independent factor to the outcome of infection with certain strains. Although the conclusions that can be drawn from these data are still limited, our findings introduce the intriguing hypothesis that advanced generational age of eukaryotic pathogens that cause chronic infection could contribute to pathogenesis. Our findings introduce a completely novel concept in pathogenesis-related research.

Senescence occurs in clonally replicating eukaryotic cells and has important implications for cells because it precedes death. Aging-related research is highly relevant for human well-being, as it is associated with the occurrence of cancer and other chronic degenerative diseases. Much of the fundamental knowledge of this process has been gained from studies with model organisms, including the unicellular budding yeast *S. cerevisiae*. Although yeast cultures appear to grow forever and seem to be immortal as long as nutrients are available, it has been established that asymmetric cell division occurs and that mother cells have a finite replicative life span (21). The mortality rate of mother cells increases exponentially with the number of cell divisions undergone (23). Life span differs for individual strains (12). Many phenotypic changes occur in generational aging, including accumulation of extrachromosomal ribosomal DNA (26) and carbonylated proteins (1) and loss of genomic stability, including an increase in recombinational events (17, 28).

Senescence is also described in filamentous ascomycetes, namely, *Podospora anserina* (24) and *Neurospora crassa* (15). *P. anserina* display a limited strain-specific life span of a few weeks. Phenotypic changes, which include a decrease in the growth rate, loss of fertility, an increase in mycelial pigmentation, and abnormal branching and swelling of hyphal tips, are seen in old cultures. Ultimately, growth of the culture ceases completely and the mycelium dies. In *N. crassa*, senescing strains usually contain intramitochondrial plasmids, which integrate into the mitochondrial DNA, causing insertional mutagenesis. This leads to functionally defective mitochondria, which spread through interconnected hyphal cells. Ultimately, the growth of a fungal colony ceases due to dysfunctional oxidative phosphorylation.

To our knowledge, this is the first report to demonstrate effects of generational aging on the phenotype of a basidiomycete, namely, *C. neoformans*. The phenotypic changes are similar to those described in *S. cerevisiae*. Specifically, we observed a size increase, a slower growth rate, and an increase in genomic instability, as evidenced by increased phenotypic switching. Although we could also identify senescent *C. albi-*

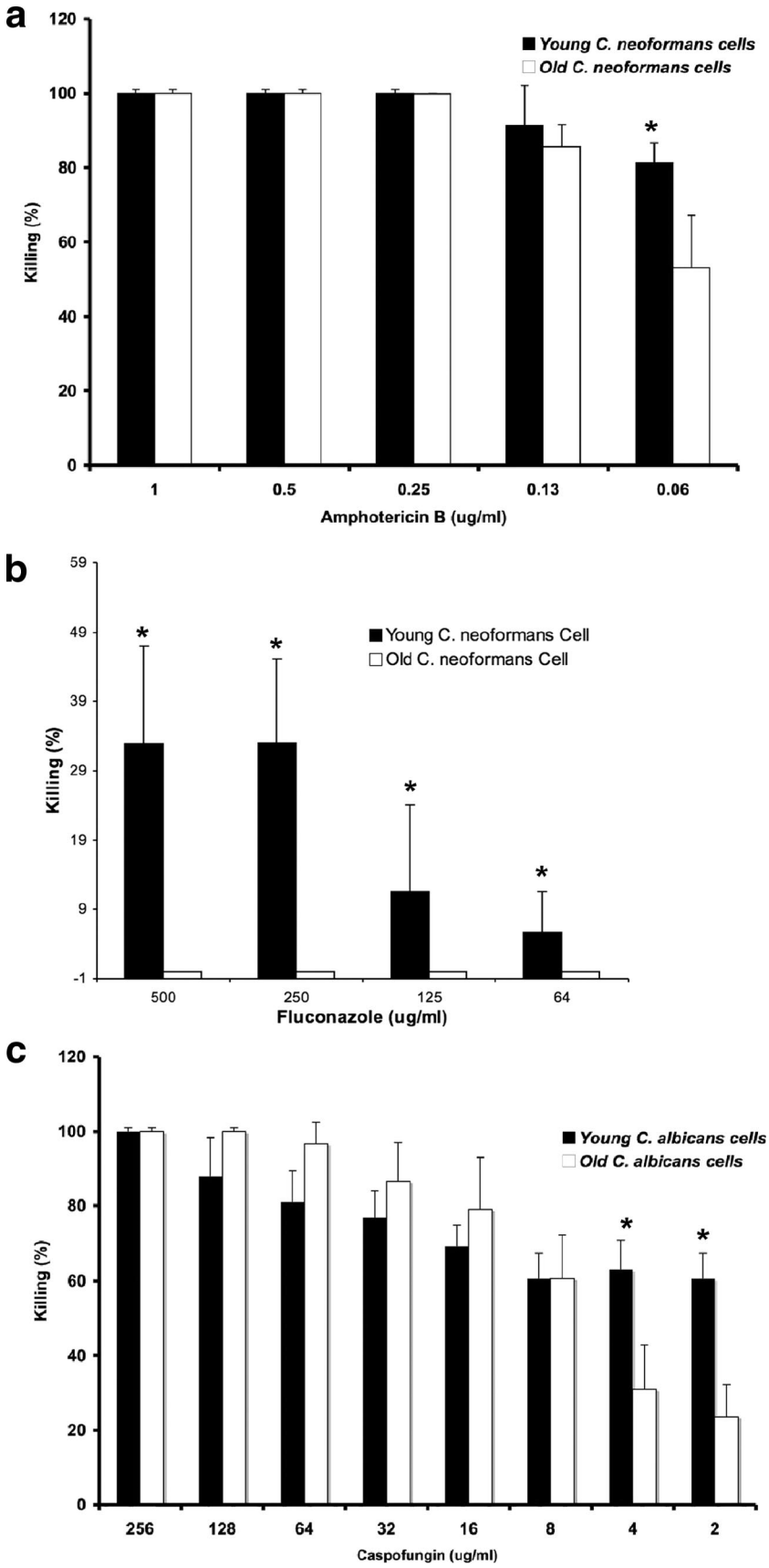

FIG. 4. Increased resistance of senescent *C. neoformans* and *C. albicans* cells in time-kill assays with antifungals. (a) Old (18 generations) *C. neoformans* cells were more resistant to killing by therapeutic doses of amphotericin B and (b) higher fluconazole doses. (c) Old (10 generations) *C. albicans* cells were also more resistant to killing by caspofungin (* represents *P* values of <0.02; experiments were done in triplicate).

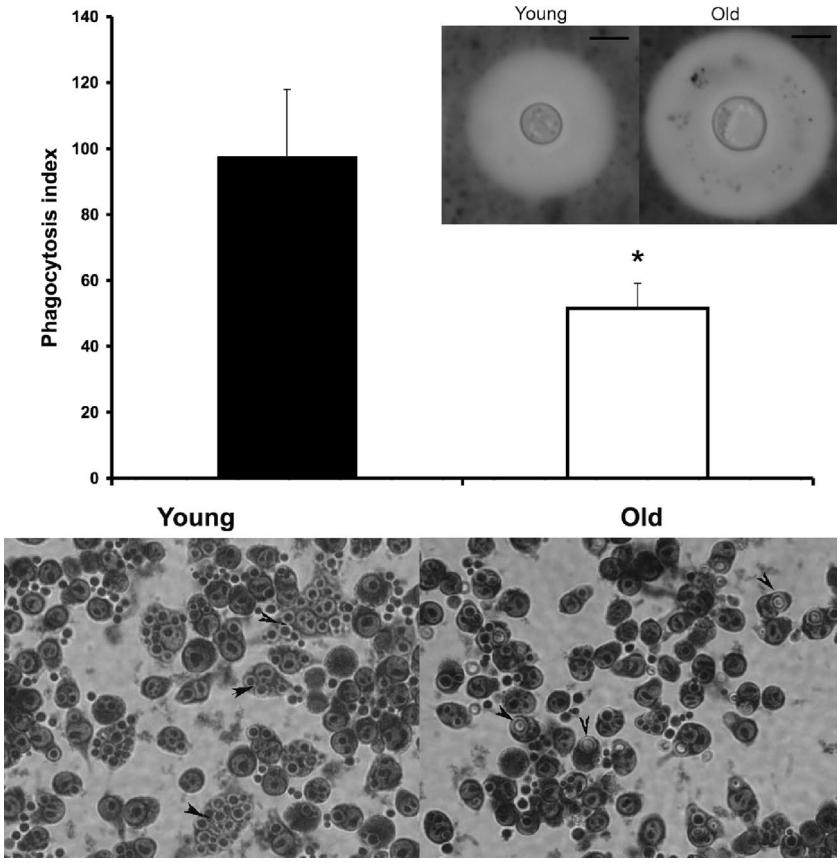

FIG. 5. Enhanced resistance of senescent *C. neoformans* cells to phagocytosis. Antibody-mediated phagocytosis of old (18 generations) *C. neoformans* cells was significantly (* represents $P < 0.05$; experiments were done in triplicate) decreased compared to that of young cells (grown overnight). In vitro capsule induction was also more pronounced in senescent *C. neoformans* cells. Bar size, 5 μm. Arrowheads indicate phagocytosis of *C. neoformans* cells by macrophages. Left, uptake of many young, small *C. neoformans* cells. Right, uptake of less old, big *C. neoformans* cells.

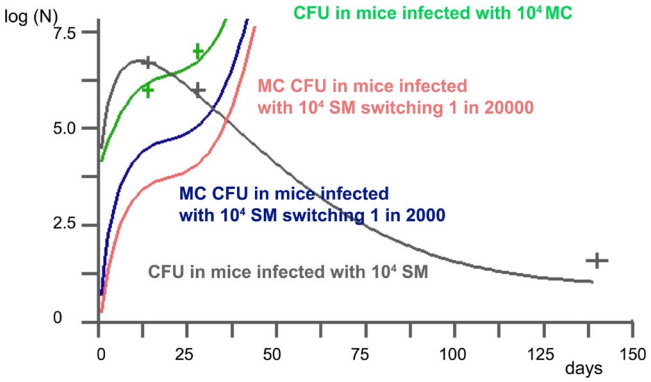

FIG. 6. Mathematical modeling of the emergence of MC variants in the setting of altered switching rates. The emergence of MC cells (CFU count in the lung, *y* axis) in mice infected with a "switching" SM strain (blue and red lines) is modeled mathematically based on experimental data. Note that, according to this model, emergence would be greatly affected by a 10-fold higher switching rate. Gray represents decreasing CFU counts of SM cells in infected mice that mount a host response. Green represents increasing CFU counts in MC cell-infected mice that cannot clear the infection.

cans cells that were increased in size, biotin labeling and isolation by magnetic column was less successful. Difficulties with biotin labeling have been reported with this fungus (16), and therefore other labeling techniques may have to be pursued in the future. Notably, we observed increased hyphal formation in older *C. albicans* cells, which could potentially affect virulence. The hyphal cell phenotype of this opportunistic pathogen interacts differently with phagocytic cells, which constitute important effector cells of the human immune response (7).

Many studies focus on how aging of the host alters its immune responses and thereby greatly affects the pathogenesis and virulence of infectious diseases (32). We asked the intriguing question whether generational aging of the pathogen can also contribute to virulence and pathogenesis of an infectious disease caused by a clonally replicating eukaryotic pathogen. Our hypothesis that an intrinsic switching rate of *C. neoformans* strain RC-2 can be augmented by generational aging was validated in vitro. We acknowledge that this finding does not prove that senescent cells accumulate and augment switching to hypervirulent variants in vivo. However, we give indirect evidence that *C. neoformans* cells from the original inoculum persist in murine infection, as they still can be found in lung homogenates after 14 and 21 days. We propose that these cells are many generations old for several reasons. First, by day 14 postinfection, the CFU count increased almost 2 logs and

based on 4-h doubling time, some cells could have doubled more than 80 times. Second, in support of ongoing replication, actively budding biotin-positive cells were seen (Fig. 3a). We do not know why biotin-positive cells in vivo were not uniformly enlarged as were cells aged in vitro (Fig. 1a). This could be a result of differential growth conditions, specifically, intra- and extracellular growth (2), which may affect size selection. Although previous studies suggested that senescent cells are less fit (25), we did not document a difference in the survival (Fig. 3b) of mice injected with young or old (24 generations) cells (median survival, 53 days versus 56 days; $P = 0.6$). We also documented that old and young cells cross the blood-brain barrier with similar frequencies despite the difference in size (Fig. 3c), which is important since the majority of chronic *C. neoformans* infections occur in the central nervous system in humans.

Within a growing *C. neoformans* population, the number of cells with advanced generational age would be very small and reduced even more if they exhibited decreased fitness. The life span of *C. neoformans* has not been established, and hence we do not know the relative age of a 20-generation-old *C. neoformans* cell. It could be that this cell still is in midlife and has reasonable fitness. Doubling time is more than doubled beyond 25 generations in the RC-2 strain but not prolonged in younger senescent cells (18 generations). The life span of *S. cerevisiae* is strain dependent and can be more than 50 generations (12). However, even if the expected number of old cells in vivo is very small, they could still affect the virulence of a pathogen population if these cells switched to hypervirulent variants. The MC phenotype is stably inherited after switching by the next generations and selected in vivo. Furthermore, our data suggest that, in vivo, the percentage of older cells could be higher than mathematically predicted if older *C. neoformans* cells gain a biological advantage through aging. We demonstrated that older cells are more resistant to killing by antifungals and to phagocytosis by macrophages. Hence, in the setting of treatment, selection could be magnified. Incidentally, this was also demonstrated for in vivo selection of switch variants in the setting of antifungal therapy (5). One would predict that in the course of chronic infection a pathogen population would shift to a population with a higher percentage of yeast cells with advanced replicative age.

The actual number of divisions that *C. neoformans* undergoes in vivo in a given time is not known. Doubling times calculated from recovered CFU do not include cells that were killed by the host response, and therefore the potential generational age distribution of cells in a population cannot be determined mathematically. Because bud scars seem to heal over, we still lack a reliable phenotypic marker that would allow us to identify senescent cells within a pathogen population in vivo. Future studies will be directed to develop methods to identify senescent cells in vivo and determine if these cells accumulate or possibly constitute a slower-growing "persister"-like cell population. The ability to sample a pathogen directly at the site of infection, namely, cerebrospinal fluid, and the availability of serial isolates from cerebrospinal fluid samples will give us a unique opportunity to investigate this dynamic microevolution within a pathogen population in a host with cryptococcal meningitis.

ACKNOWLEDGMENTS

This work was support by grant AI059681-05 to B.C.F., by pilot funds from a CFAR grant (AI 051519), and by the AIDS International Training and Research Program (Program Director, Vinayaka Prasad; NIH D43-TW001403) to I.X. and F.H. F.H. was supported by ICMR (3/1/59/MPD/2003-JRF).

We thank Xiabo Wang for technical help and Tihana Bicanic for critical reading of the manuscript.

REFERENCES

1. **Aguilaniu, H., L. Gustafsson, M. Rigoulet, and T. Nystrom.** 2003. Asymmetric inheritance of oxidatively damaged proteins during cytokinesis. Science **299:**1751–1753.
2. **Feldmesser, M., Y. Kress, and A. Casadevall.** 2001. Dynamic changes in the morphology of *Cryptococcus neoformans* during murine pulmonary infection. Microbiology **147:**2355–2365.
3. **Franzot, S., J. Mukherjee, R. Cherniak, L. Chen, J. Hamdan, and A. Casadevall.** 1998. Microevolution of standard strain of *Cryptococcus neoformans* resulting in differences in virulence and other phenotypes. Infect. Immun. **66:**89–97.
4. **Franzot, S. P., J. S. Hamdan, B. P. Currie, and A. Casadevall.** 1997. Molecular epidemiology of *Cryptococcus neoformans* in Brazil and the United States: evidence for both local genetic differences and a global clonal population structure. J. Clin. Microbiol. **35:**2243–2251.
5. **Fries, B. C., E. Cook, X. Wang, and A. Casadevall.** 2005. Effects of antifungal interventions on the outcome of experimental infections with phenotypic switch variants of *Cryptococcus neoformans*. Antimicrob. Agents Chemother. **49:**350–357.
6. **Fries, B. C., C. P. Taborda, E. Serfass, and A. Casadevall.** 2001. Phenotypic switching of *Cryptococcus neoformans* occurs in vivo and influences the outcome of infection. J. Clin. Investig. **108:**1639–1648.
7. **Gantner, B. N., R. M. Simmons, and D. M. Underhill.** 2005. Dectin-1 mediates macrophage recognition of *Candida albicans* yeast but not filaments. EMBO J. **24:**1277–1286.
8. **Goldman, D. L., B. C. Fries, S. P. Franzot, L. Montella, and A. Casadevall.** 1998. Phenotypic switching in the human pathogenic fungus *Cryptococcus neoformans* is associated with changes in virulence and pulmonary inflammatory response in rodents. Proc. Natl. Acad. Sci. USA **95:**14967–14972.
9. **Huffnagle, G. B., M. F. Lipscomb, J. A. Lovchik, K. A. Hoag, and N. E. Street.** 1994. The role of $CD4^+$ and $CD8^+$ T cells in the protective inflammatory response to a pulmonary cryptococcal infection. J. Leukoc. Biol. **55:**35–42.
10. **Jain, N., L. Li, Y. P. Hsueh, A. Guerrero, J. Heitman, D. L. Goldman, and B. C. Fries.** 2009. Loss of allergen 1 confers a hypervirulent phenotype that resembles mucoid switch variants of *Cryptococcus neoformans*. Infect. Immun. **77:**128–140.
11. **Jain, N., L. Li, D. C. McFadden, U. Banarjee, X. Wang, E. Cook, and B. C. Fries.** 2006. Phenotypic switching in a *Cryptococcus neoformans* variety *gattii* strain is associated with changes in virulence and promotes dissemination to the central nervous system. Infect. Immun. **74:**896–903.
12. **Kennedy, B. K., N. R. Austriaco, Jr., J. Zhang, and L. Guarente.** 1995. Mutation in the silencing gene SIR4 can delay aging in *S. cerevisiae*. Cell **80:**485–496.
13. **Lee, K. L., H. R. Buckley, and C. C. Campbell.** 1975. An amino acid liquid synthetic medium for the development of mycelial and yeast forms of *Candida albicans*. Sabouraudia **13:**148–153.
14. **Lockhart, S. R., K. J. Daniels, R. Zhao, D. Wessels, and D. R. Soll.** 2003. Cell biology of mating in *Candida albicans*. Eukaryot. Cell **2:**49–61.
15. **Maheshwari, R., and A. Navaraj.** 2008. Senescence in fungi: the view from Neurospora. FEMS Microbiol. Lett. **280:**135–143.
16. **Masuoka, J., L. N. Guthrie, and K. C. Hazen.** 2002. Complications in cell-surface labelling by biotinylation of *Candida albicans* due to avidin conjugate binding to cell-wall proteins. Microbiology **148:**1073–1079.
17. **McMurray, M. A., and D. E. Gottschling.** 2003. An age-induced switch to a hyper-recombinational state. Science **301:**1908–1911.
18. **McMurray, M. A., and D. E. Gottschling.** 2004. Aging and genetic instability in yeast. Curr. Opin. Microbiol. **7:**673–679.
19. **Menzel, D.** 1960. Fundamental formulas of physics, p. 734. Dover Publications, Inc., Mineola, NY.
20. **Miller, M. G., and A. D. Johnson.** 2002. White-opaque switching in *Candida albicans* is controlled by mating-type locus homeodomain proteins and allows efficient mating. Cell **110:**293–302.
21. **Mortimer, R. K., and J. R. Johnston.** 1959. Life span of individual yeast cells. Nature **183:**1751–1752.
22. **Park, B. J., K. A. Wannemuehler, B. J. Marston, N. Govender, P. G. Pappas, and T. M. Chiller.** 2009. Estimation of the current global burden of cryptococcal meningitis among persons living with HIV/AIDS. AIDS **23:**525–530.
23. **Pohley, H. J.** 1987. A formal mortality analysis for populations of unicellular

organisms (*Saccharomyces cerevisiae*). Mech. Ageing Dev. **38:**231–243.
24. **Scheckhuber, C. Q., and H. D. Osiewacz.** 2008. *Podospora anserina*: a model organism to study mechanisms of healthy ageing. Mol. Genet. Genomics **280:**365–374.
25. **Sinclair, D., K. Mills, and L. Guarente.** 1998. Aging in *Saccharomyces cerevisiae*. Annu. Rev. Microbiol. **52:**533–560.
26. **Sinclair, D. A., and L. Guarente.** 1997. Extrachromosomal rDNA circles—a cause of aging in yeast. Cell **91:**1033–1042.
27. **Slutsky, B., M. Staebell, J. Anderson, L. Risen, M. Pfaller, and D. R. Soll.** 1987. "White-opaque transition": a second high-frequency switching system in *Candida albicans*. J. Bacteriol. **169:**189–197.
28. **Smeal, T., J. Claus, B. Kennedy, F. Cole, and L. Guarente.** 1996. Loss of transcriptional silencing causes sterility in old mother cells of *S. cerevisiae*. Cell **84:**633–642.
29. **Soll, D. R.** 1992. High-frequency switching in *Candida albicans*. Clin. Microbiol. Rev. **5:**183–203.
30. **Srikantha, T., and D. R. Soll.** 1993. A white-specific gene in the white-opaque switching system of *Candida albicans*. Gene **131:**53–60.
31. **Srikantha, T., L. K. Tsai, K. Daniels, and D. R. Soll.** 2000. EFG1 null mutants of *Candida albicans* switch but cannot express the complete phenotype of white-phase budding cells. J. Bacteriol. **182:**1580–1591.
32. **van Duin, D., and A. C. Shaw.** 2007. Toll-like receptors in older adults. J. Am. Geriatr. Soc. **55:**1438–1444.
33. **Zaragoza, O., B. C. Fries, and A. Casadevall.** 2003. Induction of capsule growth in *Cryptococcus neoformans* by mammalian serum and CO_2. Infect. Immun. **71:**6155–6164.
34. **Zordan, R. E., D. J. Galgoczy, and A. D. Johnson.** 2006. Epigenetic properties of white-opaque switching in *Candida albicans* are based on a self-sustaining transcriptional feedback loop. Proc. Natl. Acad. Sci. USA **103:**12807–12812.
35. **Zordan, R. E., M. G. Miller, D. J. Galgoczy, B. B. Tuch, and A. D. Johnson.** 2007. Interlocking transcriptional feedback loops control white-opaque switching in *Candida albicans*. PLoS Biol. **5:**e256.